



CHALMERS
UNIVERSITY OF TECHNOLOGY

Probing DNA melting behaviour under vibrational strong coupling

Downloaded from: <https://research.chalmers.se>, 2025-06-07 16:46 UTC

Citation for the original published paper (version of record):

Tao, W., Mihoubi, F., Patrahau, B. et al (2025). Probing DNA melting behaviour under vibrational strong coupling. *QRB Discovery*, 6. <http://dx.doi.org/10.1017/qrd.2025.5>

N.B. When citing this work, cite the original published paper.

Probing DNA melting behaviour under vibrational strong coupling

Weijian Tao¹, Fatma Mihoubi^{1,2}, Bianca Patrahau¹, Claudia Bonfio^{1,2}, Bengt Nordén³ and Thomas W. Ebbesen¹ 

¹ISIS & icFRC, University of Strasbourg & CNRS, Strasbourg, France; ²Department of Biochemistry, University of Cambridge, Cambridge, UK and ³Department of Chemical and Biological Engineering, Chalmers University of Technology, Gothenburg, Sweden

Research Article

Cite this article: Tao W, Mihoubi F, Patrahau B, Bonfio C, Nordén B, Ebbesen TW (2025). Probing DNA melting behaviour under vibrational strong coupling. *QRB Discovery*, 6: e13, 1–7 <https://doi.org/10.1017/qrd.2025.5>.

Received: 16 December 2024
Revised: 05 February 2025
Accepted: 13 February 2025

Keywords:

DNA; light–matter interaction; melting behaviour; vibrational strong coupling; solvent

Corresponding author:

Thomas W. Ebbesen;
Email: ebbesen@unistra.fr

Abstract

Manipulating matter by strong coupling to the vacuum field has attracted intensive interests over the last decade. In particular, vibrational strong coupling (VSC) has shown great potential for modifying ground state properties in solution chemistry and biochemical processes. In this work, the effect of VSC of water on the melting behaviour of ds-DNA, an important biophysical process, is explored. Several experimental conditions, including the concentration of ds-DNA, cavity profile, solution environment, as well as thermal annealing treatment, were tested. No significant effect of VSC was observed for the melting behaviour of the ds-DNA sequence used. This demonstrates yet again the robustness of ds-DNA to outside perturbations. Our work also provides a general protocol to probe the effects of VSC on biological systems inside microfluid Fabry–Perot cavities and should be beneficial to better understand and harness this phenomenon.

Introduction

The last decade has witnessed a fast-growing interest in manipulating matter by strong coupling to the so-called vacuum electromagnetic field (Garcia-Vidal *et al.*, 2021; Nagarajan *et al.*, 2021). For instance, strong coupling between electronic transitions of molecules and optical modes has shown great potential for modifying photochemistry (Hutchison *et al.*, 2012; Zeng *et al.*, 2023), energy transport (Zhong *et al.*, 2016, 2017; Sandik *et al.*, 2025) and charge carrier conductivity (Orgiu *et al.*, 2015; Nagarajan *et al.*, 2020). On the other hand, strong coupling between vibrational transitions of molecules and the vacuum field, known as vibrational strong coupling (VSC), has also shown great potential for modifying ground-state processes, such as chemical reactivity (Thomas *et al.*, 2016; Thomas *et al.*, 2019; Pang *et al.*, 2020; Nagarajan *et al.*, 2021; Ahn *et al.*, 2023; Patrahau *et al.*, 2024), supramolecular assemblies (Hirai *et al.*, 2021; Joseph *et al.*, 2021; Sandeep *et al.*, 2022; Joseph *et al.*, 2024) and electrochemistry (Fukushima *et al.*, 2022, 2023). The strong coupling conditions are usually achieved by collective coupling of a large number (N) of molecules with an optical mode of a Fabry–Perot cavity, which gives rise to two hybrid polaritonic states (upper and lower polaritonic states, UP and LP, respectively) and N – 1 dark collective states (DS). It is important to note that strong coupling occurs even in the dark due to the involvement of the electromagnetic fluctuations of the cavity (that is, the vacuum field). VSC can be achieved either by coupling directly to the cavity a vibration of the target molecule or indirectly by the so-called cooperative coupling where solvent and solute vibrations are coupled simultaneously to the same cavity mode (Lather *et al.*, 2019; Schütz *et al.*, 2020).

In biology, VSC has also been harnessed to modify biochemical processes such as enzymatic activity in aqueous solution (Vergauwe *et al.*, 2019; Lather and George, 2021; Gao *et al.*, 2023; Gu *et al.*, 2023). The ubiquity of water as the natural medium for biological activities makes it the optimal solvent for exploring biochemical processes. Furthermore, the VSC of water is typically in the ultra-strong regime (where the energy separation of UP and LP is larger than 10% of the vibrational band) (Fukushima *et al.*, 2021; Kadyan *et al.*, 2024) and can be even observed in micro-sized water droplets without photonic structures (Canales *et al.*, 2024). Thus, water is an excellent solvent to explore VSC-induced effects in biochemical and biophysical processes.

Double-stranded deoxyribonucleic acid (ds-DNA) is a key supramolecular structure in biological systems, comprising two sequence-complementary DNA strands held together in a double helix by non-covalent interactions, e.g., hydrogen bonding between nucleotide base pairs. The non-covalent interactions provide ds-DNA high thermodynamic stability in biological environments, which is crucial for their functionalities allowing DNAs to interact with a range of biological molecules (Norden and Kurucsev, 1994; Jensen *et al.*, 1997; Vologodskii and Frank-Kamenetskii, 2018). The stability of ds-DNA helices depends among other things on the composition and sequence of the individual DNA strands, which in turn determine the

© The Author(s), 2025. Published by Cambridge University Press. This is an Open Access article, distributed under the terms of the Creative Commons Attribution-NonCommercial licence (<http://creativecommons.org/licenses/by-nc/4.0/>), which permits non-commercial re-use, distribution, and reproduction in any medium, provided the original article is properly cited. The written permission of Cambridge University Press must be obtained prior to any commercial use.

strength of several non-covalent interactions, such as hydrogen bonding, dipole–dipole, dipole-induced dipole and London dispersion forces (Devoe and Tinoco, 1962; Yakovchuk *et al.*, 2006; Vologodskii and Frank-Kamenetskii, 2018; Feng *et al.*, 2019; Nordén, 2019). The stability of ds-DNA also depends on its solvation in solution, thus sensitive to the latter's composition, salt concentration and pH (Vologodskii and Frank-Kamenetskii, 2018). The thermodynamic stability of ds-DNA can be inferred from their melting behaviour, that is, the dissociation process of ds-DNA into single-stranded (ss) DNA. As VSC has been shown to influence non-covalent interactions in chemical and biological systems (Joseph *et al.*, 2021; Sandeep *et al.*, 2022; Joseph *et al.*, 2024; Patrahau *et al.*, 2024), we sought to explore how VSC influences the stability of ds-DNA. Notably, it was recently reported that VSC affects the hybridisation process of DNA, with the thermal stability of the resulting DNA was analysed outside the optical cavity after VSC (Hou *et al.*, 2024).

Probing ds-DNA melting inside a Fabry–Perot cavity (an optical cavity consisting of two parallel mirrors) using common spectroscopy techniques remains a significant challenge due to several issues, including the limited optical pathlengths of the infrared (IR) cavities (~10 μm), the low transmission in the UV–visible region due to the metallic mirrors (less than 10%) and the low sample concentrations usually used for biological samples (1–10 μM). Therefore, employing fluorescence spectroscopy represents a promising approach, thanks to its high sensitivity. In addition, fluorescence spectroscopy based on Förster resonance energy transfer (FRET) is widely used to study biological processes (Ha, 2001; Quan *et al.*, 2020), including the denaturation of nucleic acids (Johansson *et al.*, 2002; Marras *et al.*, 2002).

In this work, we used our newly developed microfluid cavities (Patrahau *et al.*, 2024) as a platform to probe the effects of VSC on the melting behaviour of ds-DNA under equilibrium conditions. These microfluid cavities made in fused silica substrates support multiple cavity modes in the IR region and allow for sufficient light outcoupling in the UV–visible region for luminescence measurements. Additionally, they offer several advantages, such as fixed and homogeneous pathlength everywhere in the cavity with good thermal stability against temperature variations. A set of Fabry–Perot cavities with different pathlengths allows us to choose the right one for coupling the vibrational modes of water and thereby study systematically the effects induced by VSC.

Methods

Sample preparation

The DNA oligonucleotides used in this work were purchased from Integrated DNA Technologies (IDT) with HPLC purification. The sequences used for all experiments were as follows:

Strand 1: 5'-FAM-ACTCGCACCTAGT-3'.

Strand 2: 5'-ACTAGGTGCGAGT-BHQ1-3'.

where FAM and BHQ1 on strand 1 and strand 2 are, respectively, a fluorescein emitting moiety and a so-called black hole quencher. FAM was chosen as a fluorescence reporter for its high extinction coefficient (~76,900 $\text{M}^{-1}\text{cm}^{-1}$) and its near-unity fluorescence quantum yield (~0.93) (Sjöback *et al.*, 1995). BHQ-1 is a widely used quencher for FAM.

Oligonucleotides were rehydrated in Milli-Q water to a final concentration of ~500 μM . Concentrations were confirmed by UV absorbance at 260 nm using the extinction coefficients provided by IDT (141,560 $\text{M}^{-1}\text{cm}^{-1}$ for strand 1 and 138,700 $\text{M}^{-1}\text{cm}^{-1}$ for strand 2). A stock solution of ds-DNA was prepared by mixing equimolar amounts of strand 1 and strand 2 solution in a 10 mM sodium phosphate buffer (pH 7.0) in a final concentration of 10 μM . The mixture was heated between 65 and 75 $^{\circ}\text{C}$, that is, above the melting temperature estimated for the ds-DNA system ($T_m \approx 50\text{ }^{\circ}\text{C}$), for 15 min using a heating block (Thermo Fisher Scientific, Inc.). The solution was then allowed to slowly cool down to room temperature to ensure the assembly of ds-DNA. Samples were either used immediately or stored at $-4\text{ }^{\circ}\text{C}$.

To prepare 1 μM ds-DNA solution samples, the 10 μM ds-DNA stock solution was further diluted 10 times in 10 mM sodium phosphate buffer (pH 7.0). For ds-DNA samples in $\text{D}_2\text{O}/\text{H}_2\text{O}$ (90%/10%) mixed solvent, the stock solution was diluted with D_2O .

Fabry–Perot microfluid cavities

The microfluid cavities were fabricated by LioniX International and consist of fused silica substrates coated with 10 nm gold (Au) mirrors. An additional SiO_x layer (100 nm) was coated to protect the Au mirrors and to prevent any potential fluorescence quenching by physical contact with the gold. Reference structures without Au mirrors were also prepared. Schematic illustrations of the microfluid cavities and the reference structures are shown in [Supplementary Figure S1](#). More detailed descriptions about the microfluid cavities can be found in previously published work (Patrahau *et al.*, 2024).

Melting curve measurements

ds-DNA solutions were gently injected into microfluid cavities with a syringe equipped with a flat needle. The cavity was sealed at each end with round glass platelets ($\Phi = 3\text{ mm}$) and thin tape. Glue or wax as sealant was avoided not to contaminate the samples. The ds-DNA melting curve measurements inside microfluid cavities were performed in a home-built high-sensitivity fluorescence setup ([Supplementary Figure S2](#)). To perform temperature-dependent measurements, the cavities were fixed onto a commercial temperature-controlled sample holder (CD 250, Quantum Northwest, Inc., equipped with a temperature controller TC1, Quantum Northwest, Inc.). An electronically controlled optical beam shutter (SH1 and SC10, Thorlabs Inc.) was employed to minimize photobleaching and only allow laser illumination during the fluorescence measurements. Optical filters (Semrock, Inc.) optimized for the FAM fluorophore were used for collecting the signal and attenuating the excitation beam. Note that the shape of the FAM fluorescence spectrum ([Figure 1b](#)) is modified by the use of a dichroic beam-splitter with an edge at 506 nm and 540/50 nm bandpass for collection. The cutoff close to 570 nm is due to this bandpass filter.

To ensure thermal equilibrium at each temperature, cavities were held at the set temperature for 5 min before recording the emission spectrum, except when testing temperature ramping effects. By plotting the maximum emission intensity of the collected spectra as a function of temperature ([Figure 1b](#)), melting curves, as shown in [Figure 1c](#), were obtained. Measurements were repeated several times for each experimental condition to ensure reproducibility. It should be noted that the FAM emission intensity is by itself insensitive to the VSC of water. It does show a small temperature variation of about 10% ([Supplementary Figure S3](#)).

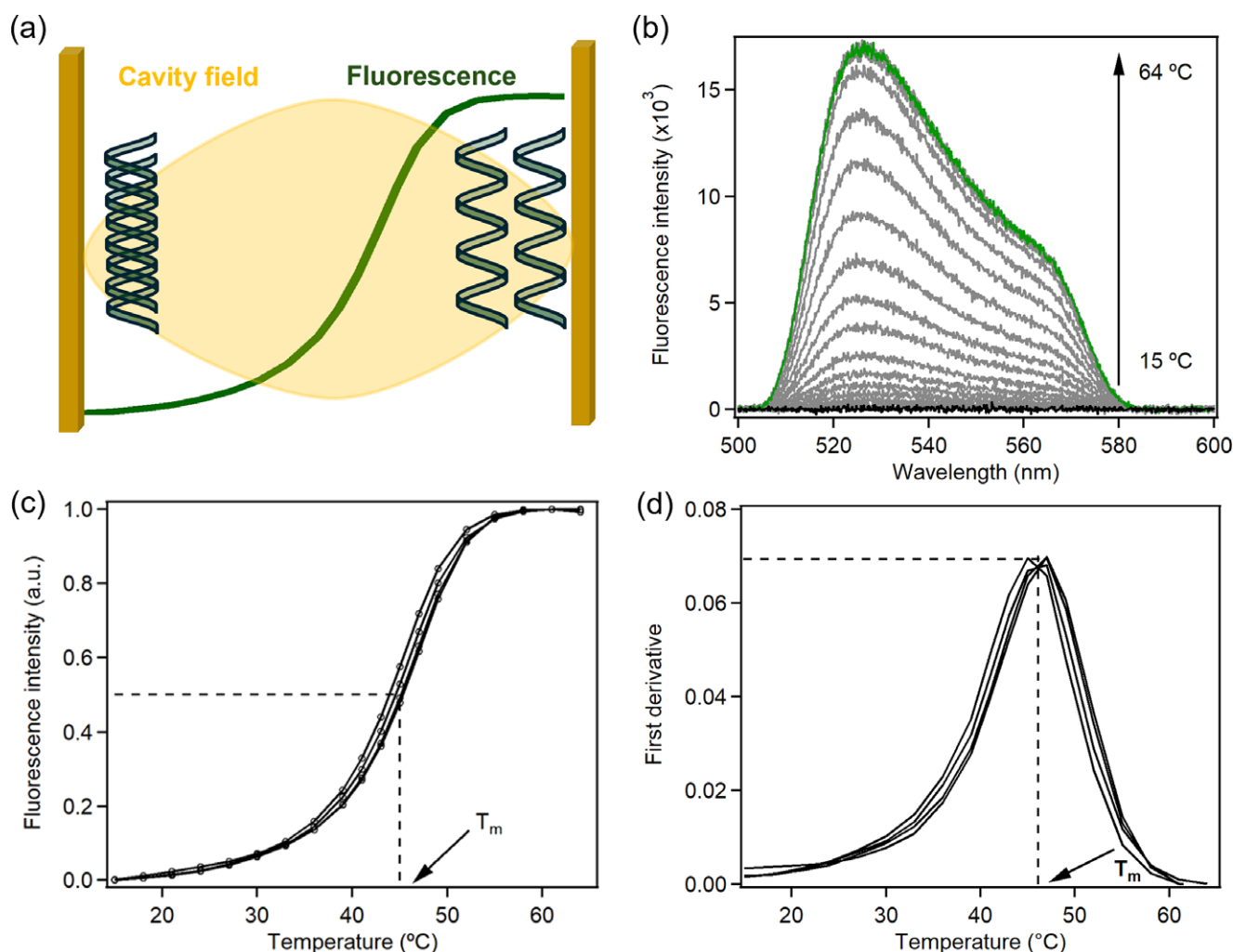


Figure 1. Principle and protocol for probing melting behaviour of ds-DNA inside the microfluidic cavity. (a) Schematic illustration of the principle of measurement based on the FRET process (yellow cavity field, green melting curve as a function of temperature). (b) Measured fluorescence spectra at different temperatures of ds-DNA at 1 μM in the reference structure (R0). (c) Extracted melting curves from four independent measurements in R0, with their corresponding first derivatives shown in (d).

Results

To begin, we established a general experimental protocol by measuring the melting curves of ds-DNA inside the reference structure R0. In the latter, the microfluidic channel is without mirrors and the two substrates are spaced by 12 μm . R0 thus acts as a control in our experiments. Figure 1a demonstrates the principle of our measurements of melting curves based on the FRET mechanism. The fluorescein (FAM) and the black hole quencher (BHQ-1) (described in the Methods section) form a FRET pair. When the two fluorophores are in proximity, as in the case of the ds-DNA involved in this study, the FAM fluorescence is quenched by BHQ-1. At high temperatures, ds-DNA disassembles into two ss-DNA oligonucleotides, and the fluorescence of FAM is restored.

A 1 μM ds-DNA solution was injected into the reference structure R0, which was fixed onto a temperature-controlled sample holder, then cooled down to 12 °C and held for an additional 1 h before measurements, thereby ensuring that all DNA was in a double-stranded state. Even then, some residual background emission can be detected with the high sensitivity of the setup. Therefore, this background spectrum collected at 12 °C was subtracted from all the spectra collected at higher temperatures. Figure 1b shows an example of fluorescence spectra measured in R0 where the

intensity increases monotonously with temperature. The emission intensities were further averaged over a large spectral range (from 510 to 550 nm), yielding the melting curves shown in Figure 1c. The intensity reaches a plateau at ca. 55 °C, suggesting that ds-DNA is dissociated into ss-DNA above this temperature. As shown in Figure 1c, the melting curves extracted from four independent measurements are superimposable, demonstrating a high reproducibility of our protocol. The melting temperature is defined as the temperature at which half of ds-DNA is dissociated into ss-DNA. To quantitatively extract the melting temperature and its standard deviation, a first-derivative analysis was performed (Owczarzy, 2005). As shown in Figure 1d, the analysis yields a melting temperature of 46.5 ± 1.0 °C for the ds-DNA for the non-optical cavity conditions of reference R0.

We then performed similar measurements with cavity S1, which has the same depth as reference structure R0, that is, 12 μm . The presence of the two gold mirrors in cavity S1 gives rise to multiple well-defined cavity modes in the infrared (IR) region, as shown in Supplementary Figure S3. The free spectral range (FSR) of cavity S1 is measured to be 415 cm^{-1} and the full width of half-maximum (FWHM) of 64 cm^{-1} , resulting in a cavity quality factor Q of 52. The eight-cavity mode at 3320 cm^{-1} indicated by the grey dashed

line in Figure 2a has a good overlap with the broad OH stretching band of water at 3300 cm^{-1} measured by attenuated total reflection (ATR) (black line in Figure 2a). After injecting the solution, two polaritonic bands emerge around the spectral region of the OH stretching band (green line in Figure 2a), with the LP band at 2922 cm^{-1} and UP band at 3683 cm^{-1} . The Rabi splitting is estimated to be $\sim 762\text{ cm}^{-1}$. The Rabi splitting is much larger than either the FWHM of the OH stretching band (445 cm^{-1}) or the FWHM of the cavity mode (64 cm^{-1}), indicating that the system under investigation entered collective VSC.

The average melting curve of ds-DNA inside cavity S1 is shown in Figure 2b, together with that obtained with the reference structure R0. As shown, no significant difference was observed between the melting curves of ds-DNA inside cavity S1 and that in R0. The first-derivate analysis gives a melting temperature of $47.0 \pm 0.0\text{ }^{\circ}\text{C}$ for the ds-DNAs inside cavity S1, which is within experimental error the same as inside the reference structure R0 ($46.5 \pm 1.0\text{ }^{\circ}\text{C}$).

To explore if cavity detuning influences the effects of VSC on the studied system, we further performed melting curve measurements (Supplementary Figure S4) and the first derivative analysis (Supplementary Figure S5) with other cavities of different FSRs and cavity profiles (cavity S2–S4, given in Table 1). However, no significant change of melting temperatures was observed across

Table 1. Melting temperatures of ds-DNA under various experimental conditions and determined by first-derivative analysis

Microfluidic cavity	Length (μm)	FSR (cm^{-1})	ds-DNA concentration (μM)	T_m ($^{\circ}\text{C}$)
R0	12.0	N/A	1	46.5 ± 1.0
S1	12.0	415	1	47.0 ± 0.0
S2	12.5	395	1	47.5 ± 1.0
S3	13.0	380	1	46.3 ± 2.3
S4	6.0	832	1	46.5 ± 1.2
R0	12.0	N/A	10	50.5 ± 2.1
S1	12.0	415	10	50.0 ± 1.7
S4	6.0	832	10	51.0 ± 1.7

different cavity detuning, as given in Table 1, and illustrated in Supplementary Figure S6.

Besides the base composition and sequence of ds-DNA, the melting behaviour of ds-DNA is also known to depend on the DNA concentration and solution composition (Vologodskii and Frank-Kamenetskii, 2018). Furthermore, recent work demonstrated that the effects of VSC on supramolecular polymerisation of porphyrins are highly dependent on concentration and solvent (Joseph *et al.*, 2024). The modification of ionic conductivity in aqueous solution through VSC was also shown to be sensitive to the composition of the electrolytes (Fukushima *et al.*, 2023). Therefore, we further extended our measurements to a concentration 10 times higher ($10\text{ }\mu\text{M}$) and also explored the effect of D_2O . As given in Table 1, the melting temperature increases at higher ds-DNA concentrations as expected (Breslauer, 1994; Vologodskii and Frank-Kamenetskii, 2018). Still, no change was observed under VSC. The corresponding melting curves of ds-DNA at $10\text{ }\mu\text{M}$ inside the reference structure R0 and two representative cavities S1 and S4 are shown in Supplementary Figure S7.

We further prepared a $1\text{ }\mu\text{M}$ ds-DNA solution in $\text{D}_2\text{O}/\text{H}_2\text{O}$ (90%/10%) mixed solvent. D_2O has stronger hydrogen bonding than H_2O , thus different solvent properties (Giubertoni *et al.*, 2023). The FTIR spectra of $\text{D}_2\text{O}/\text{H}_2\text{O}$ (90%/10%) solution in reference structure R0 and cavity S1 are shown in Figure 3a. In reference structure R0, the vibrational bands of OH stretching and OD stretching were clearly observed at 3411 and around 2500 cm^{-1} , respectively. In cavity S1, several polaritonic modes were observed due to the coupling between different cavity modes and solvent IR bands. The melting curves of ds-DNA in the mixed $\text{D}_2\text{O}/\text{H}_2\text{O}$ solution shifted to a lower temperature compared with the melting curves measured in pure H_2O solution (Figure 2b), as expected (Hou *et al.*, 2024). Once again, no significant difference was observed under VSC (Figure 3b).

During the measurement of the melting curves in the $\text{D}_2\text{O}/\text{H}_2\text{O}$ solution, we noticed that the proton exchange process between H_2O and D_2O is very slow (hour timescale) (Printz and Vonhippel, 1965). As proposed in a theoretical study, the hydration spine present in the minor groove of ds-DNA is frozen in the helix and behaves as an integral part of the double helix, which increases the thermal stability of ds-DNA (Chen and Prohofsky, 1993). The slow proton exchange indeed influenced the melting behavior of fresh and aged samples (Supplementary Figure S8).

To ensure that such a slow feature did not affect other experiments, we repeated the study of the melting curves in H_2O , first annealing the samples under VSC. The ds-DNA solution inside

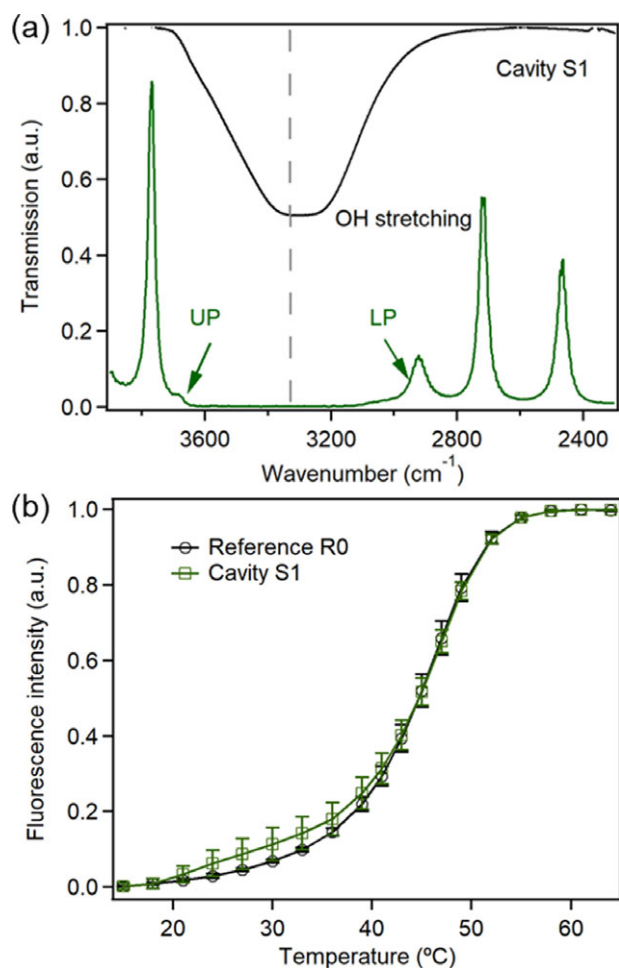


Figure 2. Melting behaviour of ds-DNA at $1\text{ }\mu\text{M}$ inside microfluidic cavities. (a) FTIR spectra of cavity S1 filled with ds-DNA solution, also shown in black line is the IR band of OH stretching mode of water. The cavity mode position is indicated in a grey-dashed line. (b) The melting curves of ds-DNA in cavity S1 and reference structure R0.

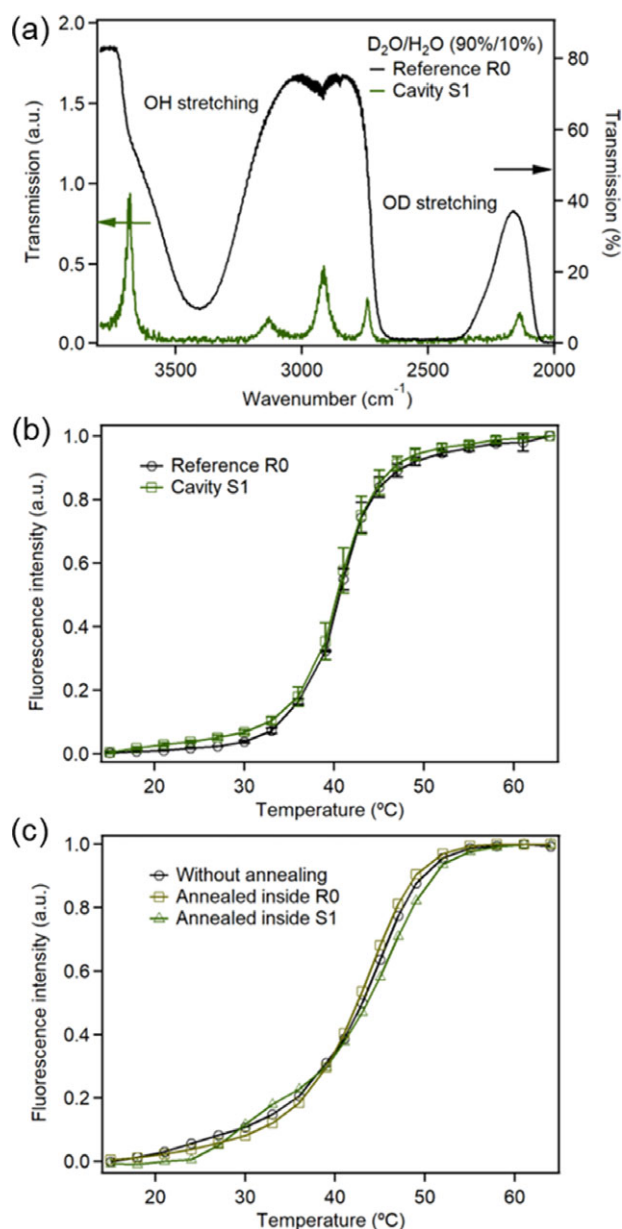


Figure 3. Melting behaviour of ds-DNA under other conditions. (a) FTIR spectrum of D₂O/H₂O (90%/10%) solution. (b) the melting curves of ds-DNA in reference structure R0 and cavity S1. (c) the melting curve after annealing in reference structure R0 and cavity S1. Also shown is the melting curve of ds-DNA without annealing in cavity S1.

microfluidic cavities was heated up to 75 °C and annealed for 1 h to fully dissociate the DNA into a single-stranded state and to fully exchange the proton between the water inside the minor grooves of ds-DNA and the solution. Then, the cavities were slowly cooled down to 12 °C and kept at that temperature for 1 h, during which time the ss-DNA re-hybridized into ds-DNA again, but under VSC. Again, this protocol did not introduce any difference in the melting temperatures of ds-DNA (Figure 3c) whether measured in the reference structure R0 or in the cavity S1.

Discussion

In summary, no significant effect from VSC on the melting curves of ds-DNA was found for all tested conditions, which included cavity

detuning, DNA concentration and solvent composition. One key difference between our work and the previous study (Hou *et al.*, 2024) is that the melting behaviour was measured in equilibrium condition in our case, while in the previous work by Hou *et al.*, it was measured in a continuous manner at a rapid ramp rate (2 °C/min). Therefore, we repeated our experiments at a similar ramp rate and without equilibrating the DNA at each temperature, but again, no significant difference was observed (Supplementary Figure S9), which further rules out the possibility of a kinetic effect from VSC in our system.

In fact, our experiments are fundamentally different from the earlier work on DNA under VSC by Hou *et al.* (2024). In that work, the ss-DNA solution was first injected into the optical cavity and the formation of ds-DNA was performed in situ at room temperature. The melting curves were then determined outside the cavity by fluorescence measurements and a decrease in T_m was found under VSC. This protocol assumes that the effects of VSC remain after extraction from the cavity. This would imply a stable structural change under VSC, which we do not detect with our DNA strand composition. In other words, it is possible that the difference in the results stems from the nucleotide composition differences in the two studies.

The insensitivity of the thermal stability of ds-DNA to VSC is in strong contrast to the supramolecular polymerisation of porphyrins, where even the relative stability between monomer and polymer can be reversibly tuned by VSC (Joseph *et al.*, 2024). The sensitivity of these porphyrin assemblies to VSC is probably due to the dynamic monomer addition and dissociation in solution and the related pathway complexity, which makes the system very sensitive to external stimuli (Mabesoone *et al.*, 2018).

The fact that we detect no effect of VSC on the melting behaviour of DNA cannot be due to a lack of cooperative coupling between the stretching mode of H₂O and the vibrational modes of DNA. The vibrational frequency of the OH stretching mode of H₂O at around 3300 cm⁻¹ is well-known to be very sensitive to the strength of hydrogen bonding (Brubach *et al.*, 2005). For liquid water, there are at least three Gaussian components within the spectral profile of the OH stretching mode at 3295, 3460, and 3590 cm⁻¹, which correspond to subpopulations of water clusters (Brubach *et al.*, 2005). The vibrational frequency of the NH stretching mode in DNA pairs also lies between 3300 and 3600 cm⁻¹ (Nir *et al.*, 2002), having a good overlap with the OH stretching mode of water. Therefore, the reason for the results must be other than an issue of cooperativity, reflecting the nature of the interaction forces at play in the DNA structure.

The thermal stability of ds-DNA is mainly determined by base-stacking interactions, which are partially from London dispersion forces and partially from hydrophobic interactions, and less by base pairing interactions, that is, hydrogen bonding (Herskovits, 1962; Yakovchuk *et al.*, 2006; Vologodskii and Frank-Kamenetskii, 2018; Feng *et al.*, 2019; Nordén, 2019). In our experiments, the water OH stretching mode is coupled to the vacuum field, where the hydrogen bonds between base pairs are also cooperatively coupled. The less important role of hydrogen bonding on the thermal stability of ds-DNA is consistent with the absence of a VSC effect. Furthermore, these hydrogen bonds are buried inside the double helix, which might also be the reason why VSC does not alter the thermal stability of ds-DNA. Therefore, our observation of the stability of ds-DNA to VSC can be considered as another new piece of evidence for the robustness of ds-DNA.

Open peer review. To view the open peer review materials for this article, please visit <http://doi.org/10.1017/qrd.2025.5>.

Supplementary material. The supplementary material for this article can be found at <http://doi.org/10.1017/qrd.2025.5>.

Data availability statement. The raw data are available upon reasonable request.

Author contribution. BN suggested the experiments. FM and CB designed the DNA sequence and prepared the corresponding samples. WT built the emission setup and carried out most of the VSC experiments. BP helped in the initial experiments. TWE supervised the project.

Financial support. We acknowledge the support from the International Center for Frontier Research in Chemistry (icFRC, Strasbourg), the Labex NIE Projects (ANR-11-LABX-0058 NIE), CSC (ANR-10-LABX-0026 CSC), USIAS (Grant No. ANR-10-IDEX-0002-02) within the Investissement d'Avenir program ANR-10-IDEX-0002-02, and the ERC (project no 788482 MOLUSC).

References

- Ahn W, Triana JF, Recabal F, Herrera F and Simpkins BS (2023) Modification of ground-state chemical reactivity via light-matter coherence in infrared cavities. *Science* **380**(6650), 1165–1168. <https://doi.org/10.1126/science.ade7147>.
- Breslauer KJ (1994) Extracting thermodynamic data from equilibrium melting curves for oligonucleotide order-disorder transitions. In Agrawal S (ed), *Protocols for Oligonucleotide Conjugates: Synthesis and Analytical Techniques*. Totowa, NJ: Humana Press, pp. 347–372.
- Brubach JB, Mermet A, Filabozzi A, Gerschel A and Roy P (2005) Signatures of the hydrogen bonding in the infrared bands of water. *The Journal of Chemical Physics* **122**(18), 184509. <https://doi.org/10.1063/1.1894929>.
- Canales A, Kotov OV, Kucukoz B and Shegai TO (2024) Self-hybridized vibrational-Mie polaritons in water droplets. *Physical Review Letters* **132**(19), 193804. <https://doi.org/10.1103/PhysRevLett.132.193804>.
- Chen YZ and Prohofsky EW (1993) Synergistic effects in the melting of DNA hydration shell: Melting of the minor groove hydration spine in poly(dA). poly(dT) and its effect on base pair stability. *Biophysical Journal* **64**(5), 1385–1393. [https://doi.org/10.1016/S0006-3495\(93\)81504-2](https://doi.org/10.1016/S0006-3495(93)81504-2).
- Devoe H and Tinoco I (1962) The stability of helical polynucleotides: Base contributions. *Journal of Molecular Biology* **4**(6), 500–517. [https://doi.org/10.1016/s0022-2836\(62\)80105-3](https://doi.org/10.1016/s0022-2836(62)80105-3).
- Feng B, Sosa RP, Martensson AKF, Jiang K, Tong A, Dorfman KD, Takahashi M, Lincoln P, Bustamante CJ, Westerlund F and Norden B (2019) Hydrophobic catalysis and a potential biological role of DNA unstacking induced by environment effects. *Proceedings of the National Academy of Sciences of the United States of America* **116**(35), 17169–17174. <https://doi.org/10.1073/pnas.1909122116>.
- Fukushima T, Yoshimitsu S and Murakoshi K (2021) Vibrational coupling of water from weak to ultrastrong coupling regime via cavity mode tuning. *Journal of Physical Chemistry C* **125**(46), 25832–25840. <https://doi.org/10.1021/acs.jpcc.1c07686>.
- Fukushima T, Yoshimitsu S and Murakoshi K (2022) Inherent promotion of ionic conductivity via collective vibrational strong coupling of water with the vacuum electromagnetic field. *Journal of the American Chemical Society* **144**(27), 12177–12183. <https://doi.org/10.1021/jacs.2c02991>.
- Fukushima T, Yoshimitsu S and Murakoshi K (2023) Unlimiting ionic conduction: Manipulating hydration dynamics through vibrational strong coupling of water. *Chemical Science* **14**(41), 11441–11446. <https://doi.org/10.1039/d3sc03364c>.
- Gao F, Guo J, Si Q, Wang L, Zhang F and Yang F (2023) Modification of ATP hydrolysis by strong coupling with O–H stretching vibration. *ChemPhotoChem* **7**(4). <https://doi.org/10.1002/cptc.202200330>.
- Garcia-Vidal FJ, Ciuti C and Ebbesen TW (2021) Manipulating matter by strong coupling to vacuum fields. *Science* **373**(6551), eabd0336. <https://doi.org/10.1126/science.abd0336>.
- Giubertoni G, Bonn M and Woutersen S (2023) D₂O as an imperfect replacement for H₂O: Problem and opportunity for protein research? *The Journal of Physical Chemistry. B* **127**, 8086–8094. <https://doi.org/10.1021/acs.jpcc.3c04385>.
- Gu KH, Si QK, Li N, Gao F, Wang LP and Zhang F (2023) Regulation of recombinase polymerase amplification by vibrational strong coupling of water. *ACS Photonics* **10**(5), 1633–1637. <https://doi.org/10.1021/acsp Photonics.3c00243>.
- Ha T (2001) Single-molecule fluorescence methods for the study of nucleic acids. *Current Opinion in Structural Biology* **11**(3), 287–292. [https://doi.org/10.1016/s0959-440x\(00\)00204-9](https://doi.org/10.1016/s0959-440x(00)00204-9).
- Herskovits TT (1962) Nonaqueous solutions of DNA: Factors determining the stability of the helical configuration in solution. *Archives of Biochemistry and Biophysics* **97**(3), 474–484. [https://doi.org/10.1016/0003-9861\(62\)90110-8](https://doi.org/10.1016/0003-9861(62)90110-8).
- Hirai K, Ishikawa H, Chervy T, Hutchison JA and Uji IH (2021) Selective crystallization via vibrational strong coupling. *Chemical Science* **12**(36), 11986–11994. <https://doi.org/10.1039/d1sc03706d>.
- Hou SJ, Gao F, Zhong CJ, Li JW, Zhu Z, Wang LP, Zhao ZX and Zhang F (2024) Vibrational alchemy of DNA: Exploring the mysteries of hybridization under cooperative strong coupling with water. *ACS Photonics* **11**(3), 1303–1310. <https://doi.org/10.1021/acsp Photonics.3c01824>.
- Hutchison JA, Schwartz T, Genet C, Devaux E and Ebbesen TW (2012) Modifying chemical landscapes by coupling to vacuum fields. *Angewandte Chemie (International Edition)* **51**(7), 1592–1596. <https://doi.org/10.1002/anie.201107033>.
- Jensen KK, Orum H, Nielsen PE and Norden B (1997) Kinetics for hybridization of peptide nucleic acids (PNA) with DNA and RNA studied with the BIAcore technique. *Biochemistry* **36**(16), 5072–5077. <https://doi.org/10.1021/bi9627525>.
- Johansson MK, Fidler H, Dick D and Cook RM (2002) Intramolecular dimers: A new strategy to fluorescence quenching in dual-labeled oligonucleotide probes. *Journal of the American Chemical Society* **124**(24), 6950–6956. <https://doi.org/10.1021/ja025678o>.
- Joseph K, de Waal B, Jansen SAH, van der Tol JJB, Vantomme G and Meijer EW (2024) Consequences of vibrational strong coupling on supramolecular polymerization of porphyrins. *Journal of the American Chemical Society* **146**(17), 12130–12137. <https://doi.org/10.1021/jacs.4c02267>.
- Joseph K, Kushida S, Smarsly E, Ihiwakrim D, Thomas A, Paravicini-Bagliani GL, Nagarajan K, Vergauwe R, Devaux E, Ersen O, Bunz UHF and Ebbesen TW (2021) Supramolecular assembly of conjugated polymers under vibrational strong coupling. *Angewandte Chemie (International Edition)* **60**(36), 19665–19670. <https://doi.org/10.1002/anie.202105840>.
- Kadyan A, Suresh MP, Johns B and George J (2024) Understanding the nature of vibro-polaritonic states in water and heavy water. *ChemPhysChem* **25**(4), e202300560. <https://doi.org/10.1002/cphc.202300560>.
- Lather J, Bhatt P, Thomas A, Ebbesen TW and George J (2019) Cavity catalysis by cooperative vibrational strong coupling of reactant and solvent molecules. *Angewandte Chemie (International Edition)* **58**(31), 10635–10638. <https://doi.org/10.1002/anie.201905407>.
- Lather J and George J (2021) Improving enzyme catalytic efficiency by co-operative vibrational strong coupling of water. *Journal of Physical Chemistry Letters* **12**(1), 379–384. <https://doi.org/10.1021/acs.jpcclett.0c03003>.
- Mabesoone MFJ, Markvoort AJ, Banno M, Yamaguchi T, Helmich F, Naito Y, Yashima E, Palmans ARA and Meijer EW (2018) Competing interactions in hierarchical porphyrin self-assembly introduce robustness in pathway complexity. *Journal of the American Chemical Society* **140**(25), 7810–7819. <https://doi.org/10.1021/jacs.8b02388>.
- Marras SAE, Kramer FR and Tyagi S (2002) Efficiencies of fluorescence resonance energy transfer and contact-mediated quenching in oligonucleotide probes. *Nucleic Acids Research* **30**(21), e122. <https://doi.org/10.1093/nar/gnf121>.
- Nagarajan K, George J, Thomas A, Devaux E, Chervy T, Azzini S, Joseph K, Jouaiti A, Hosseini MW, Kumar A, Genet C, Bartolo N, Ciuti C and Ebbesen TW (2020) Conductivity and photoconductivity of a p-type organic semiconductor under Ultrastrong coupling. *ACS Nano* **14**(8), 10219–10225. <https://doi.org/10.1021/acsnano.0c03496>.
- Nagarajan K, Thomas A and Ebbesen TW (2021) Chemistry under vibrational strong coupling. *Journal of the American Chemical Society* **143**(41), 16877–16889. <https://doi.org/10.1021/jacs.1c07420>.
- Nir E, Plützer C, Kleinerkmann K and de Vries M (2002) Properties of isolated DNA bases, base pairs and nucleosides examined by laser spectroscopy. *European Physical Journal D* **20**(3), 317–329. <https://doi.org/10.1140/epj/d/e2002-00167-2>.
- Nordén B (2019) Role of water for life. *Molecular Frontiers Journal* **03**(01), 3–19. <https://doi.org/10.1142/s2529732519400017>.

- Norden B and Kurucsev T (1994) Analysing DNA complexes by circular and linear dichroism. *Journal of Molecular Recognition* 7(2), 141–155. <https://doi.org/10.1002/jmr.300070211>.
- Orgiu E, George J, Hutchison JA, Devaux E, Dayen JF, Doudin B, Stellacci F, Genet C, Schachenmayer J, Genes C, Pupillo G, Samori P and Ebbesen TW (2015) Conductivity in organic semiconductors hybridized with the vacuum field. *Nature Materials* 14(11), 1123–1129. <https://doi.org/10.1038/nmat4392>.
- Owczarzy R (2005) Melting temperatures of nucleic acids: Discrepancies in analysis. *Biophysical Chemistry* 117(3), 207–215. <https://doi.org/10.1016/j.bpc.2005.05.006>.
- Pang Y, Thomas A, Nagarajan K, Vergauwe RMA, Joseph K, Patraha B, Wang K, Genet C and Ebbesen TW (2020) On the role of symmetry in vibrational strong coupling: The case of charge-transfer complexation. *Angewandte Chemie (International Edition)* 59(26), 10436–10440. <https://doi.org/10.1002/anie.202002527>.
- Patraha B, Piejko M, Mayer RJ, Antheaume C, Sangchai T, Ragazzon G, Jayachandran A, Devaux E, Genet C, Moran J and Ebbesen TW (2024) Direct observation of polaritonic chemistry by nuclear magnetic resonance spectroscopy. *Angewandte Chemie (International Edition)* 63(23), e202401368. <https://doi.org/10.1002/anie.202401368>.
- Printz MP and Vonhippel PH (1965) Hydrogen exchange studies of DNA structure. *Proceedings of the National Academy of Sciences of the United States of America* 53(2), 363–370. <https://doi.org/10.1073/pnas.53.2.363>.
- Quan K, Yi CP, Yang XH, He XX, Huang J and Wang KM (2020) FRET-based nucleic acid probes: Basic designs and applications in bioimaging. *Trends in Analytical Chemistry* 124, 115784. [10.1016/j.trac.2019.115784](https://doi.org/10.1016/j.trac.2019.115784).
- Sandeep K, Joseph K, Gautier J, Nagarajan K, Sujith M, Thomas KG and Ebbesen TW (2022) Manipulating the self-assembly of phenyleneethynyls under vibrational strong coupling. *Journal of Physical Chemistry Letters* 13(5), 1209–1214. <https://doi.org/10.1021/acs.jpclett.1c03893>.
- Sandik G, Feist J, Garcia-Vidal FJ and Schwartz T (2025) Cavity-enhanced energy transport in molecular systems. *Nature Materials* 24, 344–355. <https://doi.org/10.1038/s41563-024-01962-5>.
- Schütz S, Schachenmayer J, Hagenmüller D, Brennen GK, Volz T, Sandoghdar V, Ebbesen TW, Genes C and Pupillo G (2020) Ensemble-induced strong light-matter coupling of a single quantum emitter. *Physical Review Letters* 124(11), 113602. <https://doi.org/10.1103/PhysRevLett.124.113602>.
- Sjöback R, Nygren J and Kubista M (1995) Absorption and fluorescence properties of fluorescein. *Spectrochimica Acta Part A: Molecular and Biomolecular Spectroscopy* 51(6), L7–L21. [https://doi.org/10.1016/0584-8539\(95\)01421-p](https://doi.org/10.1016/0584-8539(95)01421-p).
- Thomas A, George J, Shalabney A, Dryzhakov M, Varma SJ, Moran J, Chervy T, Zhong X, Devaux E, Genet C, Hutchison JA and Ebbesen TW (2016) Ground-state chemical reactivity under vibrational coupling to the vacuum electromagnetic field. *Angewandte Chemie (International Edition)* 55(38), 11462–11466. <https://doi.org/10.1002/anie.201605504>.
- Thomas A, Lethuillier-Karl L, Nagarajan K, Vergauwe RMA, George J, Chervy T, Shalabney A, Devaux E, Genet C, Moran J and Ebbesen TW (2019) Tilting a ground-state reactivity landscape by vibrational strong coupling. *Science* 363(6427), 615–619. <https://doi.org/10.1126/science.aau7742>.
- Vergauwe RMA, Thomas A, Nagarajan K, Shalabney A, George J, Chervy T, Seidel M, Devaux E, Torbeev V and Ebbesen TW (2019) Modification of enzyme activity by vibrational strong coupling of water. *Angewandte Chemie (International Edition)* 58(43), 15324–15328. <https://doi.org/10.1002/anie.201908876>.
- Vologodskii A and Frank-Kamenetskii MD (2018) DNA melting and energetics of the double helix. *Physics of Life Reviews* 25, 1–21. <https://doi.org/10.1016/j.plrev.2017.11.012>.
- Yakovchuk P, Protozanova E and Frank-Kamenetskii MD (2006) Base-stacking and base-pairing contributions into thermal stability of the DNA double helix. *Nucleic Acids Research* 34(2), 564–574. <https://doi.org/10.1093/nar/gkj454>.
- Zeng H, Perez-Sanchez JB, Eckdahl CT, Liu P, Chang WJ, Weiss EA, Kalow JA, Yuen-Zhou J and Stern NP (2023) Control of photoswitching kinetics with strong light-matter coupling in a cavity. *Journal of the American Chemical Society* 145(36), 19655–19661. <https://doi.org/10.1021/jacs.3c04254>.
- Zhong X, Chervy T, Wang S, George J, Thomas A, Hutchison JA, Devaux E, Genet C and Ebbesen TW (2016) Non-radiative energy transfer mediated by hybrid light-matter states. *Angewandte Chemie (International Edition)* 55(21), 6202–6206. <https://doi.org/10.1002/anie.201600428>.
- Zhong X, Chervy T, Zhang L, Thomas A, George J, Genet C, Hutchison JA and Ebbesen TW (2017) Energy transfer between spatially separated entangled molecules. *Angewandte Chemie (International Edition)* 56(31), 9034–9038. <https://doi.org/10.1002/anie.201703539>.